Int. J. Solids Structures Vol. 27, No. 13, pp. 1705–1719, 1991
Printed in Great Britain

0020–7683/91 $3.00 + .00

GREEN'S FUNCTIONS OF TWO-DIMENSIONAL ANISOTROPIC PLATES CONTAINING AN ELLIPTIC HOLE

CHYANBIN HWU and WEN J. YEN
Institute of Aeronautics and Astronautics, National Cheng Kung University, Tainan, Taiwan 70101, R.O.C.

(*Received* 10 *March* 1990; *in revised form* 6 *July* 1990)

Abstract—For a two-dimensional anisotropic plate, the Green's function satisfying traction-free boundary conditions around an elliptic hole is developed using Stroh's formalism. A combination of this function and the boundary element method shows that it is the most effective approach for solving hole problems. The generality of the present Green's function is shown by the broader meaning of the following words. "Two-dimensional" includes not only in-plane but also anti-plane problems and the problems where in-plane and anti-plane deformations couple each other. "Anisotropic", which need not have any material symmetry restrictions, means that it covers the solutions given in the literature, which only deal with orthotropic or monoclinic materials. "Elliptic" includes the special case where the minor axis of the ellipse tends to zero, i.e. the case of a Griffith crack. The accuracy of the numerical method presented is then verified by comparison with exact or accepted solutions of several examples, such as an infinite or a finite plate with an elliptic hole or a crack under in-plane or anti-plane loading. The materials used are isotropic, orthotropic or laminated composites. Finally, problems where the hole boundary is not traction free are solved, such as rigid inclusions and pin-loaded holes.

INTRODUCTION

Most practical structures contain holes as parts of basic design. However, such holes cause high stress gradients, which have been studied by many investigators in the past. Analytic solutions for infinite anisotropic plates containing elliptic holes under uniform loading can be found in Savin (1961) and Lekhnitskii (1968). Due to the difficulties in satisfying the boundary conditions for finite plates, numerical methods such as the finite element and boundary element method are now widely used. The basis of the boundary element method is Green's function (or fundamental solution). The Green's function for infinite anisotropic plates was presented by Green (1941), where the boundary condition along the elliptic hole was not satisfied. In the work of Tarn and Chen (1987) and Kamel and Liaw (1989a,b), the Green's function obtained by using Lekhnitskii's approach was improved in order to satisfy the elliptic hole boundary condition. Nevertheless, the solutions obtained are valid only for monoclinic materials and in-plane loading.

In this paper, the Green's function satisfying the traction-free condition on an elliptic hole in an infinite anisotropic plate is derived in closed and compact form using Stroh's formalism (Stroh, 1958; Hwu and Ting, 1989). The derivation is valid for general anisotropic materials which need not have any material symmetry restrictions. The out-of-plane components of displacements and stresses are generally nonzero in Stroh's formalism. Hence the present solutions are valid not only for plane problems but also for anti-plane problems and problems whose in-plane and anti-plane deformations couple each other. By letting the minor axis of the elliptic hole tend to zero, the Green's function for the corresponding crack problems and its associated stress intensity factors are obtained explicitly.

A boundary element method employing the Green's function derived in this paper is used to analyze the stress distribution of finite plates containing traction-free elliptic holes. The boundary conditions along the elliptic hole are satisfied by the Green's function so that it is unnecessary to include the elliptic surface in the boundary integration. This explains why the present method is more effective than other numerical schemes. This concept has been widely used in the analysis of isotropic or anisotropic plates with cracks (Snyder and Cruse, 1975; Cruse, 1978; Murakami, 1978; Clements and Haselgrove, 1983; Ang and

Clements, 1986, 1987; Ang, 1987; Tan and Bigelow, 1988). Although the boundary-Galerkin approach (Grannel and Dwyer, 1987) also satisfies the field equations *a priori*, it remains to satisfy all the boundary conditions approximately including the elliptic hole or cracks.

To show the generality and accuracy of the numerical procedure presented here, comparisons are made with exact or accepted solutions of several examples such as an infinite or a finite plate with an elliptic hole or a crack under in-plane or anti-plane loadings. The materials used are isotropic, orthotropic or laminated composites. The elastic constants for isotropic materials give rise to the degenerate case where some of the constants in the Green's function are ill-defined. To employ the present Green's function for the degenerate case, a small perturbation of the material constants is introduced.

We also examine problems where elliptic holes are filled with rigid inclusions or loaded by pins. For the rigid inclusion problem, we employ Green's function satisfying zero displacements on the boundary of the inclusion (assuming that there is symmetry such that any relative rotation can be neglected) so that, as for the traction-free hole problem, there is no need to perform integration over the boundary of the inclusion. By careful superposition of stresses, the numerical procedure for the traction-free hole problem can be used to solve the pin-loaded hole problem. Numerical results for various specific problems are obtained.

GREEN'S FUNCTION FOR TRACTION-FREE HOLE PROBLEM

In a fixed rectangular coordinate system x_i, $i = 1, 2, 3$, let u_i and σ_{ij} be the displacement and stress, respectively. The strain–displacement equations, the stress–strain laws and the equations of equilibrium are

$$\varepsilon_{ij} = \tfrac{1}{2}(u_{i,j} + u_{j,i}), \tag{1}$$

$$\sigma_{ij} = C_{ijks}\varepsilon_{ks}, \tag{2}$$

$$C_{ijks}u_{k,sj} = 0, \tag{3}$$

where repeated indices imply summation, a comma stands for differentiation and the C_{ijks} are elastic constants which are assumed to be fully symmetric and positive definite. For two-dimensional problems u_i, $i = 1, 2, 3$, can be assumed to depend on x_1 and x_2 only. Based on this assumption and the basic equations (1)–(3), the general solutions for u_i and σ_{ij} can then be written as (Stroh, 1958; Hwu and Ting, 1989)

$$\mathbf{u} = 2\,\mathrm{Re}\left\{\sum_{\alpha=1}^{3}\mathbf{a}_\alpha f_\alpha(z_\alpha)\right\}, \quad \boldsymbol{\phi} = 2\,\mathrm{Re}\left\{\sum_{\alpha=1}^{3}\mathbf{b}_\alpha f_\alpha(z_\alpha)\right\}, \tag{4}$$

$$\sigma_{i1} = -\phi_{i,2}, \quad \sigma_{i2} = \phi_{i,1}, \tag{5}$$

where Re denotes the real part of a complex number, and $\mathbf{u}$ and $\boldsymbol{\phi}$ are 3×1 matrices whose elements are u_i and ϕ_i, $i = 1, 2, 3$. ϕ_i represents the stress function which can be used to determine stresses according to (5). $f_\alpha(z_\alpha)$ is an arbitrary function of the complex variable z_α $(= x_1 + p_\alpha x_2)$, the choice of which depends on the boundary conditions provided by the given problems. The eigenvalues p_α and the associated eigenvectors $\mathbf{a}_\alpha$, $\mathbf{b}_\alpha$ are determined by the elasticity constants C_{ijks} (Hwu and Ting, 1989). Note that the solutions given in (4) are derived under the assumption that the p_α, $\alpha = 1, 2, 3$, are distinct.

Considering an infinite anisotropic plate containing an elliptic hole under a concentrated force $\mathbf{f}$ applied at point $\mathbf{x}^* = (x_1^*, x_2^*)$, as shown in Fig. 1, the elasticity solution of this problem will be used as a Green's function of the boundary element method (BEM).

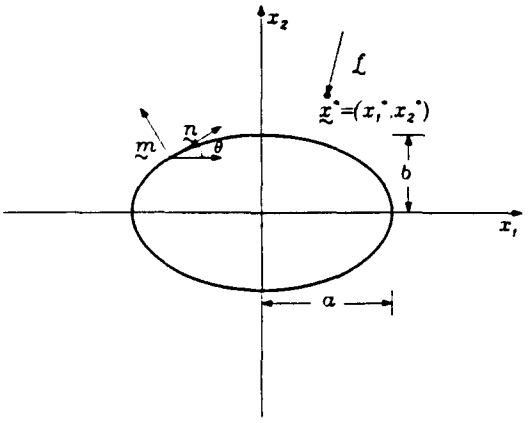

Fig. 1. An infinite anisotropic plate containing an elliptic hole under a concentrated force **f** applied at point $\mathbf{x}^* = (x_1^*, x_2^*)$.

If the hole is assumed to be traction free, the boundary conditions can be written as

$$\begin{aligned} &\mathbf{t}_m = \boldsymbol{\phi}_{,n} = \mathbf{0} \text{ along the hole boundary,} \\ &\int_C \mathrm{d}\boldsymbol{\phi} = \mathbf{f} \text{ for any closed curve } C \text{ enclosing the point } \mathbf{x}^*, \\ &\sigma_{ij} \to 0 \text{ at infinity,} \end{aligned} \tag{6}$$

where $\mathbf{t}_m$ is the surface traction along the hole boundary of which the normal is $\mathbf{m}$. The equality between $\mathbf{t}_m$ and $\boldsymbol{\phi}_{,n}$ was proved by Stroh (1958), where $\mathbf{n}$ is tangent to the boundary (Fig. 1). The second equation of (6) comes from the force equilibrium around any closed curve enclosing point $\mathbf{x}^*$ and the use of eqn (5).

To satisfy (6), the choice of $f_k(z_\alpha)$ becomes critical in the solution procedures. As in the problem considered by Hwu and Ting (1989), a mapping function which transforms an ellipse into a circle will be used to satisfy $(6)_1$. The second equation of (6) implies that $\boldsymbol{\phi}$ must be a multi-valued function around the point $\mathbf{x}^*$; however, its derivatives which are related to the stresses should be single valued and approach zero when $|z| \to \infty$. The best candidate for satisfying these conditions, the second and third eqns of (6), is the logarithmic function. Hence, a possible general solution of displacements and stress functions can be written as

$$\begin{aligned} \mathbf{u} &= 2 \sum_{k=0}^{3} \mathrm{Re}\,\{\mathbf{A}\mathbf{F}_k(\mathbf{Z})\mathbf{q}_k\}, \\ \boldsymbol{\phi} &= 2 \sum_{k=0}^{3} \mathrm{Re}\,\{\mathbf{B}\mathbf{F}_k(\mathbf{Z})\mathbf{q}_k\}, \end{aligned} \tag{7}$$

where

$$\mathbf{A} = [\mathbf{a}_1 \quad \mathbf{a}_2 \quad \mathbf{a}_3], \quad \mathbf{B} = [\mathbf{b}_1 \quad \mathbf{b}_2 \quad \mathbf{b}_3], \tag{8}$$

$$\mathbf{F}_k(\mathbf{Z}) = \mathrm{diag}\,[f_k(z_1), \ f_k(z_2), \ f_k(z_3)], \quad k = 0, 1, 2, 3 \tag{9}$$

and

$$\begin{aligned} f_0(z_\alpha) &= \log(\zeta_\alpha - \zeta_\alpha^*), \\ f_k(z_\alpha) &= \log(\zeta_\alpha^{-1} - \bar{\zeta}_k^*), \quad k = 1, 2, 3 \end{aligned} \tag{10}$$

$$\zeta_\alpha = \frac{z_\alpha + \sqrt{z_\alpha^2 - a^2 - p_\alpha^2 b^2}}{a - ip_\alpha b},$$

$$\zeta_\alpha^* = \frac{z_\alpha^* + \sqrt{z_\alpha^{*2} - a^2 - p_\alpha^2 b^2}}{a - ip_\alpha b}, \tag{11}$$

where $\alpha = 1, 2, 3$ and a, b are the length of the semi-axes of the ellipse, $\mathbf{q}_k$ are 3×1 matrices whose elements are unknown complex constants determined by the satisfaction of the boundary conditions (6). Note that the additional terms $f_1(z_\alpha)$, $f_2(z_\alpha)$, $f_3(z_\alpha)$ are chosen in order to satisfy the traction-free condition along the hole boundary. The overbar denotes the complex conjugate.

To determine $\mathbf{q}_k$ by using (6), we need to calculate $\boldsymbol{\phi}_{,n}$ along the hole boundary of which the contour is represented by

$$x_1 = a \cos \psi, \quad x_2 = b \sin \psi. \tag{12}$$

In the above, ψ is related to θ, which is the angle directed from the x_1-axis to the tangent $\mathbf{n}$, by

$$\rho \cos \theta = a \sin \psi, \quad \rho \sin \theta = -b \cos \psi, \tag{13}$$

where

$$\rho^2 = a^2 \sin^2 \psi + b^2 \cos^2 \psi. \tag{14}$$

Using the chain rule, we have

$$\frac{\partial f}{\partial n} = \frac{\partial f}{\partial \zeta_\alpha} \frac{\partial \zeta_\alpha}{\partial \psi} \frac{\partial \psi}{\partial z_\alpha} \left[\frac{\partial z_\alpha}{\partial x_1} \frac{\partial x_1}{\partial n} + \frac{\partial z_\alpha}{\partial x_2} \frac{\partial x_2}{\partial n} \right], \tag{15}$$

where

$$\zeta_\alpha = e^{i\psi}, \quad \frac{\partial \zeta_\alpha}{\partial \psi} = i e^{i\psi}, \quad \frac{\partial z_\alpha}{\partial \psi} = -\rho(\cos \theta + p_\alpha \sin \theta), \quad \frac{\partial x_1}{\partial n} = \cos \theta, \quad \frac{\partial x_2}{\partial n} = \sin \theta,$$

$$\frac{\partial z_\alpha}{\partial x_1} = 1, \quad \frac{\partial z_\alpha}{\partial x_2} = p_\alpha,$$

along the hole boundary. Substituting the above results into (9) and (10), we obtain

$$\mathbf{F}_{0,n} = \operatorname{diag} [c_1 \quad c_2 \quad c_3] = \sum_{k=1}^{3} c_k \mathbf{I}_k,$$
$$\mathbf{F}_{k,n} = \bar{c}_k \mathbf{I}, \quad k = 1, 2, 3, \tag{16}$$

where

$$c_k = \frac{-i e^{i\psi}}{\rho(e^{i\psi} - \zeta_k^*)} \tag{17}$$

and

$$\mathbf{I}_1 = \begin{bmatrix} 1 & 0 & 0 \\ 0 & 0 & 0 \\ 0 & 0 & 0 \end{bmatrix}, \quad \mathbf{I}_2 = \begin{bmatrix} 0 & 0 & 0 \\ 0 & 1 & 0 \\ 0 & 0 & 0 \end{bmatrix}, \quad \mathbf{I}_3 = \begin{bmatrix} 0 & 0 & 0 \\ 0 & 0 & 0 \\ 0 & 0 & 1 \end{bmatrix}. \tag{18}$$

$\mathbf{I}$ is the 3×3 unit matrix. By using (16), $\boldsymbol{\phi}_n$ can easily be calculated from $(7)_2$, and the boundary condition $(6)_1$ will be satisfied if we choose

$$\mathbf{q}_k = -\mathbf{B}^{-1}\bar{\mathbf{B}}\mathbf{I}_k\bar{\mathbf{q}}_0, \quad k = 1,2,3. \tag{19}$$

The force equilibrium equation $(6)_2$ and the requirement of single-valued displacement will now provide

$$\begin{aligned} 2\,\mathrm{Re}\,\{\mathrm{i}\mathbf{B}\mathbf{q}_0\} &= \mathbf{f}/2\pi, \\ 2\,\mathrm{Re}\,\{\mathrm{i}\mathbf{A}\mathbf{q}_0\} &= \mathbf{0}. \end{aligned} \tag{20}$$

In the above, (7) and the multi-valuedness of $\log(\zeta_\alpha - \zeta_\alpha^*)$ have been used. It is noted that $\log(\zeta_\alpha^{-1} - \bar{\zeta}_k^*)$ is single valued since ζ_α^{-1} is always located inside the unit circle and $\bar{\zeta}_k^*$ is a point outside the unit circle. To find $\mathbf{q}_0$ from (20), we recall the orthogonality relations among the eigenvectors (Stroh, 1958; Ting, 1988),

$$\begin{bmatrix} \mathbf{A}^{\mathrm{T}} & \mathbf{B}^{\mathrm{T}} \\ \bar{\mathbf{A}}^{\mathrm{T}} & \bar{\mathbf{B}}^{\mathrm{T}} \end{bmatrix} \begin{bmatrix} \mathbf{B} & \bar{\mathbf{B}} \\ \mathbf{A} & \bar{\mathbf{A}} \end{bmatrix} = \mathbf{I}$$

and obtain

$$\mathbf{q}_0 = \mathbf{A}^{\mathrm{T}}\mathbf{f}/2\pi\mathrm{i}. \tag{21}$$

Substituting (19) and (21) into (7), the Green's function can then be written explicitly as

$$\begin{aligned} \mathbf{u} &= \frac{1}{\pi}\,\mathrm{Im}\,\{\mathbf{A}\mathbf{F}_0(\mathbf{Z})\mathbf{A}^{\mathrm{T}}\}\mathbf{f} + \frac{1}{\pi}\sum_{k=1}^{3}\mathrm{Im}\,\{\mathbf{A}\mathbf{F}_k(\mathbf{Z})\mathbf{B}^{-1}\bar{\mathbf{B}}\mathbf{I}_k\bar{\mathbf{A}}^{\mathrm{T}}\}\mathbf{f}, \\ \boldsymbol{\phi} &= \frac{1}{\pi}\,\mathrm{Im}\,\{\mathbf{B}\mathbf{F}_0(\mathbf{Z})\mathbf{A}^{\mathrm{T}}\}\mathbf{f} + \frac{1}{\pi}\sum_{k=1}^{3}\mathrm{Im}\,\{\mathbf{B}\mathbf{F}_k(\mathbf{Z})\mathbf{B}^{-1}\bar{\mathbf{B}}\mathbf{I}_k\bar{\mathbf{A}}^{\mathrm{T}}\}\mathbf{f}, \end{aligned} \tag{22}$$

where Im denotes the imaginary part of a complex number.

The Green's function for an infinite anisotropic plate containing a crack of length $2a$ can be obtained by letting $b \to 0^+$ in (22). Differentiating the stress function $\boldsymbol{\phi}$ in (22) with respect to x_1 and considering $x_2 = 0$, $x_1 > a$, the stresses σ_{i2} ahead of the crack tip along the x_1 axis are obtained as

$$\boldsymbol{\sigma}_2 = \frac{1}{\pi a}\left\{1 + \frac{x_1}{\sqrt{x_1^2 - a^2}}\right\}\mathrm{Im}\left\{\sum_{\alpha=1}^{3}\left(\frac{1}{\zeta - \zeta_\alpha^*} + \frac{1}{\zeta - \zeta^2\zeta_\alpha^*}\right)\mathbf{b}_\alpha\mathbf{a}_\alpha^{\mathrm{T}}\right\}\mathbf{f}, \tag{23}$$

where

$$\zeta = \frac{1}{a}(x_1 + \sqrt{x_1^2 - a^2}), \quad \zeta_\alpha^* = \frac{1}{a}(z_\alpha^* + \sqrt{z_\alpha^{*2} - a^2}). \tag{24}$$

and

$$\boldsymbol{\sigma}_2 = \{\sigma_{21}, \sigma_{22}, \sigma_{23}\}^{\mathrm{T}}. \tag{25}$$

With the usual definition and use of (23), the stress intensity factors are given by

$$\mathbf{K} = \begin{Bmatrix} K_{II} \\ K_I \\ K_{III} \end{Bmatrix} = \lim_{x_1 \to a} \sqrt{2\pi(x_1 - a)}\sigma_2$$

$$= \frac{2}{\sqrt{\pi a}} \operatorname{Im}\{\mathbf{B}\boldsymbol{\Psi}(\mathbf{Z}^*)\mathbf{A}^{\mathrm{T}}\}\mathbf{f}. \tag{26}$$

where

$$\boldsymbol{\Psi}(\mathbf{Z}^*) = \operatorname{diag}\left\{\frac{1}{1-\zeta_1^*}, \frac{1}{1-\zeta_2^*}, \frac{1}{1-\zeta_3^*}\right\}. \tag{27}$$

If the point force $\mathbf{f}$ is applied to the upper crack surface $x_1 = c$, eqn (26) becomes

$$\mathbf{K} = \frac{-1}{2\sqrt{\pi a}}\mathbf{S}^{\mathrm{T}}\mathbf{f} + \frac{1}{2\sqrt{\pi a}}\left(\frac{a+c}{a-c}\right)^{1/2}\mathbf{f}, \tag{28}$$

where the identity $\mathbf{S} = \mathrm{i}(2\mathbf{A}\mathbf{B}^{\mathrm{T}} - \mathbf{I})$ (Barnett and Lothe, 1973; Ting, 1988) has been used and $\mathbf{K}$ is identical to the solution given by Wu (1989).

BOUNDARY ELEMENT METHOD

Boundary integral equation

If body forces are omitted, the boundary integral equation is written as (Brebbia *et al.*, 1984)

$$c_{ij}(\mathbf{x}^*)u_j(\mathbf{x}^*) + \int_{B+L} p_{ij}^*(\mathbf{x}^*, \mathbf{x})u_j(\mathbf{x})\,\mathrm{d}\Gamma(\mathbf{x}) = \int_{B+L} u_{ij}^*(\mathbf{x}^*, \mathbf{x})p_j(\mathbf{x})\,\mathrm{d}\Gamma(\mathbf{x}), \tag{29}$$

where $u_{ij}^*(\mathbf{x}^*, \mathbf{x})$ and $p_{ij}^*(\mathbf{x}^*, \mathbf{x})$ are, respectively, the displacements and tractions in the j direction at a point $\mathbf{x}$ corresponding to a unit point force acting in the i direction applied at a point $\mathbf{x}^*$ and B, L denote the contour of the outer and hole boundary. For a smooth boundary $c_{ij} = \frac{1}{2}\delta_{ij}$, in which δ_{ij} is the Kronecker delta. For practical application, however, c_{ij} together with the corresponding principal value can be indirectly computed by letting $u_j = 1$ (and hence $p_j = 0$) in eqn (29).

For the traction-free hole problem, we choose u_{ij}^* and p_{ij}^* in such a way that $p_{ij}^* = 0$ on the elliptic boundary L. Then, by applying the boundary condition $p_j = 0$ on L, we find that

$$\int_L p_{ij}^*(\mathbf{x}^*, \mathbf{x})u_j(\mathbf{x})\,\mathrm{d}\Gamma(\mathbf{x}) = \int_L u_{ij}^*(\mathbf{x}^*, \mathbf{x})p_j(\mathbf{x})\,\mathrm{d}\Gamma(\mathbf{x}) = 0. \tag{30}$$

Similarly, for the rigid inclusion problem, assuming that there is no relative rotation between the matrix and inclusion, if $u_{ij}^* = 0$ on L, eqn (30) is also valid.

Linear elements are used here to solve the boundary integral equation. A detailed discussion of the numerical implementation of this element can be found in Brebbia *et al.* (1984). The boundary B is discretized into M elements with N nodes. For a boundary with n corner nodes, $M = N - n$ because each corner node connects two different surfaces which have two different tractions and should be represented by two nodes. In each node one of the two variables (u_i or p_i) is known. By considering $\mathbf{x}^*$ as boundary point, eqn (29) finally

reduces to a system of $3N$ simultaneous linear algebraic equations. The integrals including the one with a singular term are calculated using Gauss quadrature rules.

Once all the values of tractions and displacements on the boundary are determined, the values of the stresses and displacements at any interior point can be calculated by using (29) again, where $c_{ij} = \delta_{ij}$. But now, $\mathbf{x}^*$ denotes the interior point, $u_j(\mathbf{x})$, $p_j(\mathbf{x})$ are all known from previous calculations and u_{ij}^*, p_{ij}^* are given by the Green's function. The displacements at the interior point $u_j(\mathbf{x}^*)$ are then obtained directly from (29). To find the internal stresses, we firstly calculate $u_{j,i}(\mathbf{x}^*)$ by differentiating (29) with respect to $\mathbf{x}^*$, then apply (1) to get the strains and (2) to get the stresses.

Examples

(1) *A finite or an infinite plate with an elliptic hole*

A uniform tension of $\sigma_0 = 1$ GPa is applied in x_2 direction. The material constants of the orthotropic plate are taken as

$$E_1 = 11.8\,\text{GPa}, \quad E_2 = 5.9\,\text{GPa}, \quad G_{12} = 0.69\,\text{GPa}, \quad \nu_{12} = 0.071,$$

where the fiber direction is denoted by 1. The lamina angle α is 90°, where α is measured from the x_1-axis to the fiber direction. Because of eqn (30), only the external boundary needs to be discretized. An infinite plate containing a circular hole is simulated by defining $b/a = 1$, $2a/W = 0.01$, $H/W = 3$ (Fig. 2). A very coarse mesh is employed in this case with four elements on each edge. Therefore, 20 nodes for the entire plate are required. Results for the hoop stress $\sigma_{\theta\theta}$ are shown in Table 1. We observed that there is a very good agreement between the analytic (Lekhnitskii, 1968) and computed solution by the boundary element method.

The main concern in the following cases is the stress concentration factor (SCF), which is defined by $\sigma_{\theta\theta}/\sigma_0$ at point A. The SCF is presented in Fig. 3 for a variety of b/a ratios in order to investigate the effect of the shape of an elliptic hole on the stress concentration factor, where $2a/W = 0.2$, $H/W = 3$ and $\alpha = 90°$. The results of Fig. 3 show that the larger the b/a ratio, the smaller the stress concentration factor, which is expected. The relation between the SCF and lamina angle α is shown in Fig. 4.

(2) *A circular rigid inclusion in an infinite plate*

The geometry, loading and material properties for this case are the same as for the above problem except that the circular hole is replaced with a circular rigid inclusion. Therefore, the boundary condition $\phi_{,n} = 0$ is now replaced by $\mathbf{u} = 0$ without considering the relative rotation between the matrix and rigid inclusion due to the symmetry condition

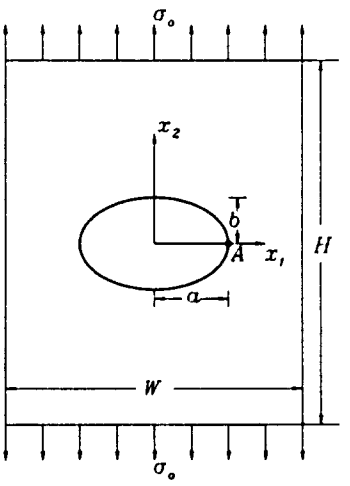

Fig. 2. A finite plate containing an elliptic hole.

Table 1. The hoop stress $\sigma_{\theta\theta}$ on the boundary of a circular hole in an infinite plate (simulated by $b/a = 1$, $2a/W = 0.01$, $H/W = 3$).

θ(Degree)	Present	Exact
0.0	5.466	5.453
15.	2.565	2.571
30.	0.962	0.964
45.	0.403	0.404
60.	0.070	0.069
75.	-0.339	-0.340
90.	-0.707	-0.707

of this case. The Green's function of this problem has a similar form to (22) except that $\mathbf{B}^{-1}\bar{\mathbf{B}}$ are now changed to $\mathbf{A}^{-1}\bar{\mathbf{A}}$. The results for the stresses are compared with the exact solutions (Lekhnitskii, 1968) and are shown in Table 2.

(3) *A composite laminate with a center crack under uniform tension*

The geometry and loading for this problem are as shown in Fig. 2 with $b \to 0^+$, $H/W = 3$. Numerical results are obtained for three laminates: $(90^\circ)_s$, $(\pm 30^\circ)_s$, $(0^\circ/\pm 45^\circ/90^\circ)_s$, which are relevant to application to composite structures. The material properties of each lamina are denoted by

$$E_1 = 114.8\,\text{GPa}, \quad E_2 = E_3 = 11.72\,\text{GPa}, \quad G_{12} = G_{13} = G_{23} = 9.65\,\text{GPa},$$
$$\nu_{12} = \nu_{13} = \nu_{23} = 0.21.$$

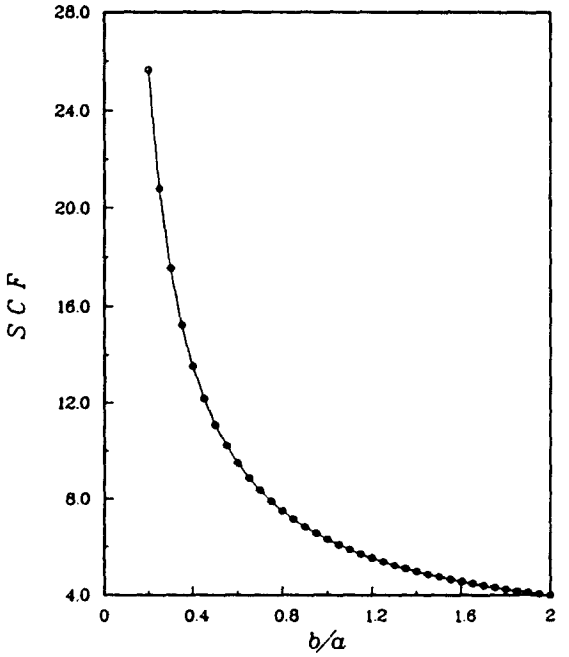

Fig. 3. The effect of the shape of an elliptic hole on the stress concentration factor (SCF).

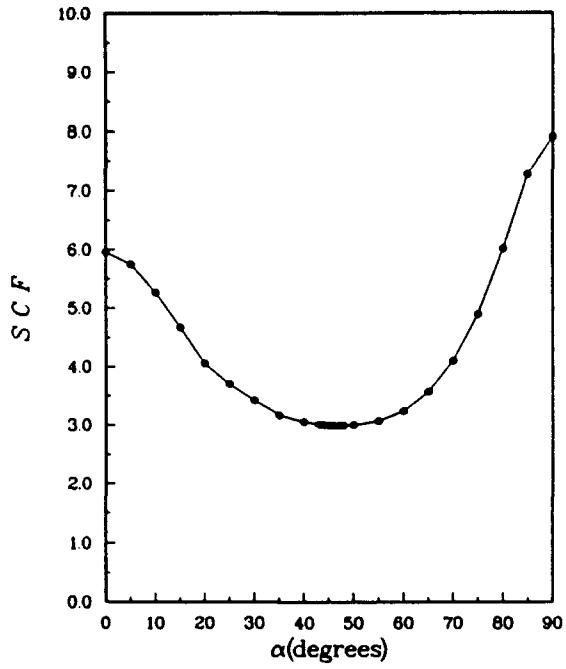

Fig. 4. The relation between the stress concentration factor (SCF) and the lamina angle α.

To study the effects of the specimen boundary, the results are presented using the stress-intensity correction factor (F)

$$F = \frac{K_I}{\sigma\sqrt{\pi a}}.$$

Figure 5 shows that the stress-intensity correction factors calculated by this method agree, within $\pm 1\%$, with the values from Snyder and Cruse (1975).

(4) *An orthotropic plate with a center crack under anti-plane loading*

A mode III problem is now considered to show the generality of this method. An infinite plate is simulated by defining $2a/W = 0.01$ in Fig. 6. The plate is sheared by a stress

Table 2. The stresses on the boundary of a circular rigid inclusion in an infinite plate (simulated by $b/a = 1$, $2a/W = 0.01$, $H/W = 3$).

	σ_{rr}/σ_0		$\sigma_{r\theta}/\sigma_0$		$\sigma_{\theta\theta}/\sigma_0$	
θ(Degree)	Present	Exact	Present	Exact	Present	Exact
0.0	0.038	0.04	0.	0.	0.003	0.
15.	0.118	0.20	-0.299	-0.30	0.563	0.56
30.	0.336	0.34	-0.517	-0.52	0.698	0.70
45.	0.635	0.64	-0.597	-0.60	0.514	0.52
60.	0.934	0.94	-0.517	-0.52	0.269	0.27
75.	1.157	1.16	-0.292	-0.30	0.096	0.09
90.	1.233	1.24	0.	0.	0.047	0.04

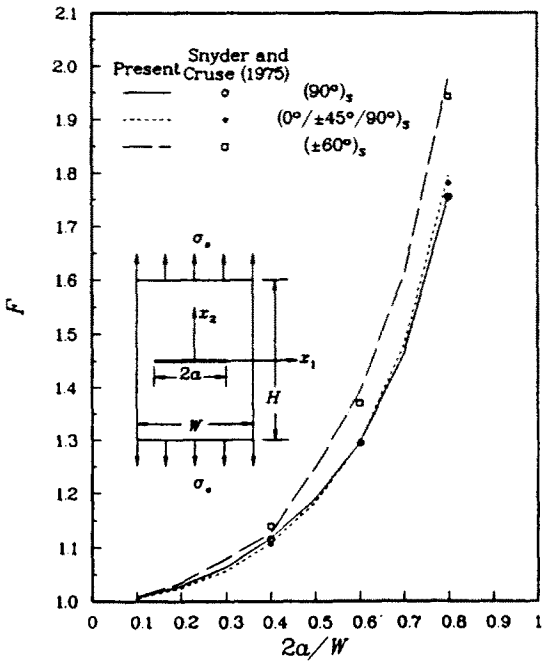

Fig. 5. The stress-intensity correction factor (F) for a center-crack tension specimen ($H/W = 3.0$).

$\sigma_{21} = \tau$ on $x_2 = \pm H/2$. For orthotropic materials, we take the lamina properties considered in Example 3 and orient the fiber direction to the x_1-axis. The stress-intensity factor K_{III} calculated converges to $1.001\tau\sqrt{\pi a}$, which shows that it is not influenced by material properties for small cracks.

(5) *An isotropic plate with a rigid line inclusion under uniform tension*

Since the eigenvalues p_α, $\alpha = 1, 2, 3$, are repeated and equal to i for isotropic materials (Lekhnitskii, 1968), eqn (4) is no longer true. However, the generality of the present method can be extended by introducing a small perturbation in the values of p_α such as $p_1 = 0.9952i$, $p_2 = i$, $p_3 = 1.0048i$. Similar to Example 2, the Green's function for rigid line inclusions should be revised by replacing $\mathbf{B}^{-1}\bar{\mathbf{B}}$ with $\mathbf{A}^{-1}\bar{\mathbf{A}}$ and letting $b \to 0^+$. For an infinite isotropic plate subjected to a tensile loading σ perpendicular to the line inhomogeneity (length $2a$), the mode I stress singularity coefficient S_I defined by Wang *et al.* (1985) is given as

$$S_I = \sigma\sqrt{\pi a}\,\frac{(\kappa-1)(3-\kappa)}{8\kappa}, \tag{31}$$

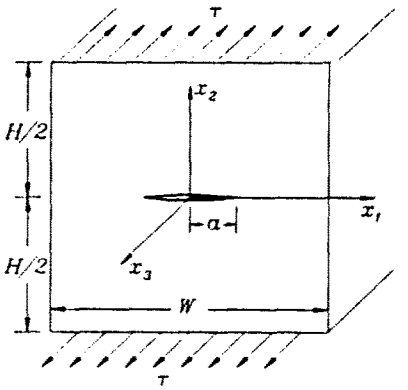

Fig. 6. A plate containing a crack under anti-plane shear loading ($H/W = 1$).

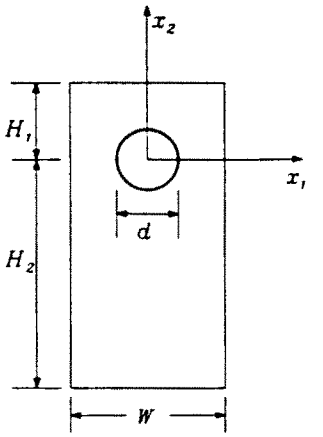

Fig. 7. The geometry of Examples 6 and 7 ($H_1/d = 2.5$, $H_2/d = 7.5$, $W/d = 5$).

where $\kappa = 3-4\nu$ for plane strain deformation. The present numerical solution, based upon $2a/W = 0.01$, $\nu = 0.071$ and the perturbation given above, converges to $0.02241\sigma\sqrt{\pi a}$, which is almost identical to the exact solution given in (31).

(6) *A finite plate with a pin-loaded hole*

A finite plate with a hole is shown in Fig. 7, which is subjected to a uniform tension applied at $x_2 = -H_2$. The material constants of the orthotropic plate are taken as

$$E_1 = 10\,\text{GPa}, \quad E_2 = 10\,\text{GPa}, \quad G_{12} = 10/3.3\,\text{GPa}, \quad \nu_{12} = 0.25.$$

A cosine normal load distribution is assumed here to simulate a pin-loaded hole (Chang *et al.*, 1983; Vable and Sikarskie, 1988). The pressure around the upper half of the hole boundary induced by a unit stress applied in the x_2 direction can then be expressed as

$$\sigma_{nn} = P\cos\theta^*,$$

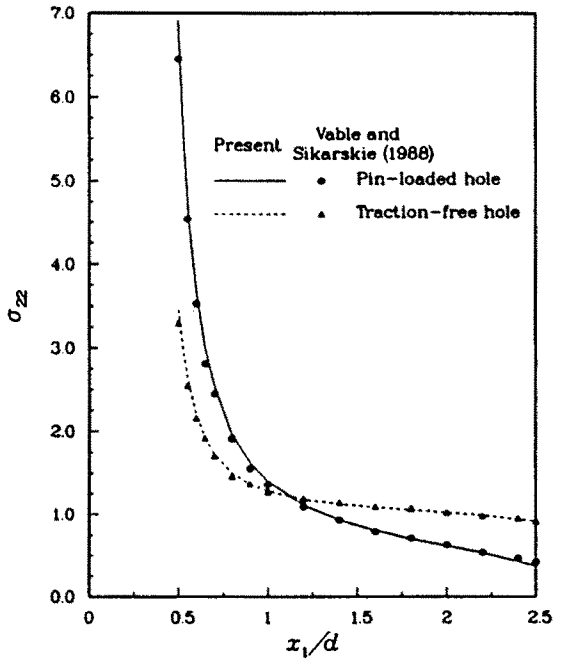

Fig. 8. Normal stress (σ_{22}) along the x_1-axis.

Table 3. The total force along the x_1-axis.

Problem	Present	Vable (1988)	Exact
6	5.004	4.993	5.000
7	5.012	4.937	5.000

where θ^* is measured clockwise from the x_2 axis, $\mathbf{m}$ is the direction normal to hole boundary, and P is determined by the equilibrium condition that the total forces in the vertical direction balance, i.e.

$$2\int_0^{\pi/2}(P\cos^2\theta^*)\frac{\mathrm{d}}{2}\mathrm{d}\theta^* = \frac{\pi}{4}Pd = 1\times W.$$

From the above equation, P is given by $4W/\pi d$. The Green's function derived in this paper is under the condition that the hole is free of traction. In order to solve the problem with the load distribution described above, superposition of the following two problems is employed. One is an infinite plate with $\sigma_{mm} = (4W/\pi d)\cos\theta^*$ applied on the upper half of the hole boundary, which can be solved analytically (see the Appendix). The other is a finite plate (Fig. 7) for which the loadings applied on the outer and hole boundaries are obtained from those of the original problem minus the above one. Therefore, the loading on the hole boundary is traction free so that it can be solved by the present boundary element method. The results for normal stress σ_{22} along the x_1 axis are shown and compared in Fig. 8. The results for the total force along the x_1 axis are shown in Table 3.

(7) *Convergency and accuracy*

A sample problem dealing with a traction-free hole under uniaxial tension given in Vable and Sikarskie (1988), Fig. 7, is used to study the convergency and accuracy of the present method. A uniform tension is applied at $x_2 = H_1$ and $-H_2$. All the other boundaries including the circular hole boundary are traction free and the material properties are the same as in Example 6. The effect of varying N (the number of nodes) on the stress concentration factor is shown in Table 4. A good convergence rate is observed from $N = 8$ to $N = 42$. The results for normal stress σ_{22} along the positive x_1 axis are shown in Fig. 8. By static equilibrium the area under the curve shown in Fig. 8 represents half the total force applied in the x_2 direction, which is shown in Table 3.

CONCLUSIONS

The Green's function of an anisotropic plate containing an elliptic hole is obtained in closed and compact form by using Stroh's formalism. The Green's function for the traction-free hole problem is such that, in applying the boundary element method, discretization around the boundary of the hole is avoided. This results in a saving of computer time and storage. Moreover, discretization with relatively coarse meshes can achieve high accuracy.

Several examples such as isotropic, orthotropic or laminated composite plates with an elliptic hole or a crack under in-plane or anti-plane loadings were considered, to show the general applicability of Green's function presented in this paper. Accuracy and convergency

Table 4. The effect of varying N (the number of nodes) on the stress concentration factor.

N	8	10	12	14	18	24	32	42
S C F	2.917	3.282	3.368	3.404	3.413	3.434	3.461	3.466

have been shown through comparison with the exact or accepted solutions given in the literature. Additional examples are given for problems where the hole boundary is not traction free, such as a rigid inclusion or pin-loaded hole. The former is accomplished by using a Green's function satisfying the condition of zero displacement on the boundary of the inclusion. By careful superposition of the linear stresses, the latter can be solved using the numerical procedure for the traction-free hole problem.

REFERENCES

Ang, W. T. (1987). A boundary integral equation for deformations of an elastic body with an arc crack. *Q. Appl. Math.* **45**, 131–139.

Ang, W. T. and Clements, D. L. (1986). A boundary element method for determining the effect of holes on the stress distribution around a crack. *Int. J. Numer. Meth. Engng* **23**, 1727–1737.

Ang, W. T. and Clements, D. L. (1987). A boundary integral equation method for the solution of a class of crack problems. *J. Elasticity* **17**, 9–21.

Barnett, D. M. and Lothe, J. (1973). Synthesis of the sextic and the integral formalism for dislocation, Green's function and surface waves in anisotropic elastic solids. *Phys. Norv.* **7**, 13–19.

Brebbia, C. A., Telles, J. C. F. and Wrobel, L. C. (1984). *Boundary Element Techniques*. Springer, New York.

Chang, F.-K., Scott, R. A. and Springer, G. S. (1983). Strength of mechanically fastened composite joints. *J. Comp. Mater.* **16**, 470–494.

Clements, D. L. and Haselgrove, M. A. (1983). A boundary integral equation for a class of crack problems in anisotropic elasticity. *Int. J. Comp. Math.* **12**, 267–278.

Cruse, T. A. (1978). Two-dimensional BIE fracture mechanics analysis. *Appl. Math. Modeling* **2**, 287–293.

Grannel, J. J. and Dwyer, J. (1987). A boundary-Galerkin edge-function approach to anisotropic elasticity. In *BEM IX* (Edited by Brebbia, L. A., Wendland, W. L. and Kuhn, G). Computational Mechanics, Southampton.

Green, A. E. (1941). A note on stress systems in aelotropic materials. *Phil. Mag.* **34**, 416–418.

Hwu, C. and Ting, T. C. T. (1989). Two-dimensional problems of the anisotropic elastic solid with an elliptic inclusion. *Q. J. Mech. Appl. Math.* **42**, 553–572.

Kamel, M. and Liaw, B. M. (1989a). Green's functions due to concentrated moments applied in an anisotropic plane with an elliptic hole or a crack. *Mech. Res. Communs* **16**(5), 311–319.

Kamel, M and Liaw, B. M. (1989b). Analysis of a loaded elliptical hole or crack in an anisotropic plane. *Mech. Res. Communs* **16**(6), 379–383.

Lekhnitskii, S. G. (1968). *Anisotropic Plates*. Gordon and Breach, New York.

Murakami, Y. (1978). Application of the body force method to the calculation of stress intensity factors for a crack in an arbitrarily shaped plate. *Engng Fracture Mech.* **10**, 497–513.

Savin, G. N. (1961). *Stress Concentration Around Holes*. Pergamon Press, London.

Snyder, M. D. and Cruse, T. A. (1975). Boundary-integral equation analysis of cracked anisotropic plates. *Int. J. Fracture* **11**, 315–328.

Stroh, A. N. (1958). Dislocations and cracks in anisotropic elasticity. *Phil. Mag.* **7**, 625–646.

Tan, P. W. and Bigelow, C. A. (1988). Analysis of cracked laminates with holes using the boundary force method. *AIAA* **26**, 1094–1099.

Tarn, J. Q. and Chen, T. C. (1987). Optimized shape of notch in plates subjected to inplane loading via boundary element method. M.S. Thesis, Department of Civil Engineering, NCKU, Taiwan.

Ting, T. C. T. (1988). Some identities and the structure of N_1 in the Stroh formalism of anisotropic elasticity. *Q. Appl. Math.* **46**, 109–120.

Vable, M. and Sikarskie, D. L. (1988). Stress analysis in plane orthotropic material by the boundary element method. *Int. J. Solids Structures* **24**, 1–11.

Wang, Z. Y., Zhang, H. T. and Chou, Y. T. (1985). Characteristics of the elastic field of a rigid line inhomogeneity. *J. Appl. Mech.* **52**, 818–822.

Wu, K. C. (1989). Representations of stress intensity factors by path-independent integrals. *J. Appl. Mech.* **56**, 780–785.

APPENDIX: ANALYTICAL SOLUTIONS FOR AN ANISOTROPIC PLATE WITH AN ELLIPTIC OPENING SUBJECTED TO ARBITRARY LOADINGS

Any given arbitrary loadings applied on the hole boundary can be expressed by Fourier expansion as

$$\rho \mathbf{t}_m = \mathbf{c}_0 + \sum_{k=1}^{n} (\mathbf{c}_k \cos k\psi + \mathbf{d}_k \sin k\psi), \tag{A1}$$

where

$$\mathbf{c}_0 = \frac{1}{2\pi}\int_{-\pi}^{\pi} \rho \mathbf{t}_m \, d\psi,$$

$$\mathbf{c}_k = \frac{1}{\pi}\int_{-\pi}^{\pi} \rho \mathbf{t}_m \cos k\psi \, d\psi,$$

$$\mathbf{d}_k = \frac{1}{\pi}\int_{-\pi}^{\pi} \rho \mathbf{t}_m \sin k\psi \, d\psi, \tag{A2}$$

and

$$\rho^2 = a^2 \sin\psi + b^2 \cos^2\psi. \tag{A3}$$

To satisfy the above boundary condition, the stress function ϕ can be assumed as

$$\phi = 2\,\mathrm{Re}\{\mathbf{B}\mathbf{F}_0(\mathbf{Z})\mathbf{q}_0\} + 2\sum_{k=1}^{\infty}\mathrm{Re}\{\mathbf{B}\mathbf{F}_k(\mathbf{Z})\mathbf{q}_k\}, \tag{A4}$$

where

$$\begin{aligned}\mathbf{F}_0(\mathbf{Z}) &= \mathrm{diag}[\log\zeta_1,\ \log\zeta_2,\ \log\zeta_3],\\ \mathbf{F}_k(\mathbf{Z}) &= \mathrm{diag}[\zeta_1^{-k},\ \zeta_2^{-k},\ \zeta_3^{-k}].\end{aligned} \tag{A5}$$

The traction $\mathbf{t}_m$ along the hole boundary can then be calculated by $\mathbf{t}_m = \phi_{,n}$. Differentiation with respect to n is performed by using chain rule given in (15). To get a real form expression, we replace the complex constant $\mathbf{q}_k$ by

$$\mathbf{q}_k = \mathbf{A}^{\mathrm{T}}\mathbf{g}_k + \mathbf{B}^{\mathrm{T}}\mathbf{h}_k, \quad k = 0, 1, 2, \ldots, \infty, \tag{A6}$$

where $\mathbf{g}_k$ and $\mathbf{h}_k$ are real. Using the following three real matrices (Barnett and Lothe, 1973),

$$\mathbf{S} = \mathrm{i}(2\mathbf{A}\mathbf{B}^{\mathrm{T}} - \mathbf{I}), \quad \mathbf{H} = 2\mathrm{i}\mathbf{A}\mathbf{A}^{\mathrm{T}}, \quad \mathbf{K} = -2\mathrm{i}\mathbf{B}\mathbf{B}^{\mathrm{T}}, \tag{A7}$$

the traction $\mathbf{t}_m$ along the hole boundary is now obtained as

$$\rho\mathbf{t}_m = -(\mathbf{S}^{\mathrm{T}}\mathbf{g}_0 - \mathbf{L}\mathbf{h}_0) + \sum_{k=1}^{\infty} k\{(\mathbf{S}^{\mathrm{T}}\mathbf{g}_k - \mathbf{L}\mathbf{h}_k)\cos k\psi + \mathbf{g}_k \sin k\psi\}. \tag{A8}$$

A comparison between (A1) and (A8) leads to

$$\begin{aligned}\mathbf{S}^{\mathrm{T}}\mathbf{g}_0 - \mathbf{L}\mathbf{h}_0 &= -\mathbf{c}_0,\\ \mathbf{S}^{\mathrm{T}}\mathbf{g}_k - \mathbf{L}\mathbf{h}_k &= \frac{1}{k}\mathbf{c}_k,\\ \mathbf{g}_k &= \frac{1}{k}\mathbf{d}_k, \quad k = 1, 2, \ldots, \infty.\end{aligned} \tag{A9}$$

The requirement of a single-valued displacement gives

$$2\,\mathrm{Re}\{\mathrm{i}\mathbf{A}\mathbf{q}_0\} = \mathbf{H}\mathbf{g}_0 + \mathbf{S}\mathbf{h}_0 = \mathbf{0}. \tag{A10}$$

Combining (A9) and (A10), we obtain

$$\begin{aligned}\mathbf{g}_0 &= \mathbf{S}^{\mathrm{T}}\mathbf{c}_0, \quad \mathbf{h}_0 = \mathbf{H}\mathbf{c}_0,\\ \mathbf{g}_k &= \frac{1}{k}\mathbf{d}_k, \quad \mathbf{h}_k = \frac{1}{k}\mathbf{L}^{-1}(\mathbf{S}^{\mathrm{T}}\mathbf{d}_k - \mathbf{c}_k), \quad k = 1, 2, \ldots, \infty.\end{aligned} \tag{A11}$$

For the pin-loaded hole considered in Example 6,

$$\begin{aligned}\mathbf{t}_m &= P\cos\theta^*\begin{Bmatrix}\sin\theta^*\\ \cos\theta^*\\ 0\end{Bmatrix} = P\begin{Bmatrix}\sin\psi\cos\psi\\ \sin^2\psi\\ 0\end{Bmatrix}, \quad 0 \leqslant \psi \leqslant \pi,\\ &= \mathbf{0}, \quad \pi \leqslant \psi \leqslant 2\pi.\end{aligned} \tag{A12}$$

From (A2) and (A3) with $a = b = d/2$, we have

$$\begin{aligned}\mathbf{c}_0 &= \frac{\mathrm{d}P}{4\pi}\begin{Bmatrix}0\\ \pi/2\\ 0\end{Bmatrix},\\ \mathbf{c}_k &= \frac{\mathrm{d}P}{4\pi}\begin{Bmatrix}\dfrac{4}{4-k^2}\\ 0\\ 0\end{Bmatrix}, \quad k = \text{odd},\\ &= \mathbf{0}, \quad k = \text{even except 2}.\end{aligned}$$

$$= \frac{dP}{4\pi}\begin{Bmatrix} 0 \\ -\pi/2 \\ 0 \end{Bmatrix}, \quad k = 2,$$

$$\mathbf{d}_k = \frac{dP}{4\pi}\begin{Bmatrix} 0 \\ \dfrac{8}{k(4-k^2)} \\ 0 \end{Bmatrix}, \quad k = \text{odd},$$

$$= \mathbf{0}, \quad k = \text{even except 2},$$

$$= \frac{dP}{4\pi}\begin{Bmatrix} \pi/2 \\ 0 \\ 0 \end{Bmatrix}, \quad k = 2. \tag{A13}$$